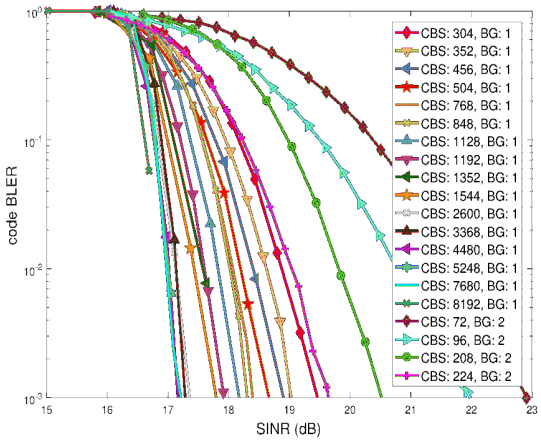

Fig. 3: code BLER vs SINR (dB) for MCS23 of MCS Table1.

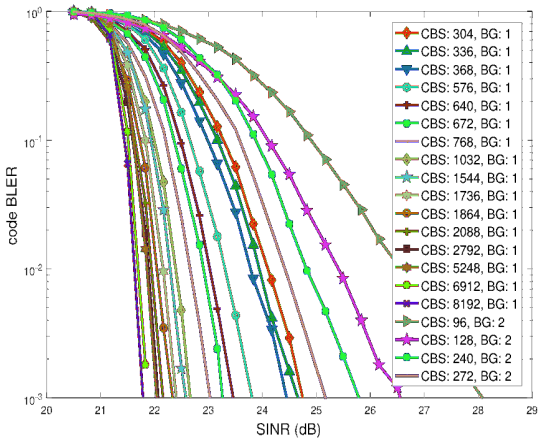

Fig. 4: code BLER vs SINR (dB) for MCS21 of MCS Table2.

Due to space constraints we cannot include all the SINR-code BLER curves in this paper, instead, we only show the results for two specific MCS indices, i.e., MCS23 of MCS Table1 in Fig. 3 and MCS21 of MCS Table2 in Fig. 4. The data for all the curves can be found in the ns-3 based NR SLS [12] (https://5g-lena.cttc.es). For each case, different CBSs are simulated, and for each CBS, the selected BG type is indicated in the legend. Note that because MCS23 of MCS Table1 is equivalent to MCS16 of MCS Table2, therefore, the range of SINRs in Fig. 3 is lower than the SINR range of Fig. 4. As it can be seen from the plots, the CBS has a high impact on the actual BLER performance for a given MCS, which was observed also in LTE [2]. As the CBS increases, it provides better code BLER performance for a fixed SINR.

Note that the SINR-code BLER curves obtained from LLS are quantized and consider a subset of CBSs. Accordingly, in the SLS, we implement a worst case approach to determine the code BLER value by using lower bounds of the actual CBS and effective SINR. In the PHY abstraction for HARQ-IR, for simplicity and according to the obtained curves, we limit the effective ECR in Eq. (3) by the lowest ECR of the MCSs that have the same modulation order as the selected MCS index.

D. Transport BLER computation

As mentioned in the previous section, each baseline SINR-BLER curve was estimated without code block segmentation in the LLS, ensuring that the transport BLER was equal to the code BLER. However, in the SLS, we simulate TBSs that may require code block segmentation. Therefore, there is a need to convert the code BLER found from the LLS's lookup table to the transport BLER for the given TBS.

The code BLERs of the C code blocks (as determined by the code block segmentation described in Section III-A) are combined to get the BLER of a transport block as:

$$\text{TBLER} = 1 - \prod_{i=1}^{C}(1 - \text{CBLER}_i) \approxeq 1 - (1 - \text{CBLER})^C, \quad (6)$$

where the last approximate equality holds because code block segmentation in NR generates code blocks of roughly equal sizes[1].

IV. End-to-End Evaluation in ns-3

As previously mentioned, the PHY abstraction model proposed in Section III has been integrated into an NR based SLS, particularly in the NR SLS of the popular and open-source ns-3 [12], thus giving life and promoting the use of the proposed model. In this section, an end-to-end evaluation to illustrate the usability of the model is performed. Different sets of NR configurations are used, including fixed MCS, adaptive MCS, different HARQ methods (HARQ-CC and HARQ-IR), and the two NR MCS tables (MCS Table1 and Table2).

A. Simulation Scenario

We consider a gNB-UE link in an Urban Micro scenario with 28 GHz carrier frequency, SCS of 120 kHz, and 100 MHz channel bandwidth. For the simulations, the gNB-UE 2D distance is varied (within values 10m, 30m, 50m, 70m) to emulate different channel qualities. The heights of the gNB and the UE are set to 10 m and 1.5 m, respectively. The fast fading based 3GPP channel model [16] is used. Uniform planar arrays are used for both the gNB and the UE. The number of antennas is set to 4×8 at the gNB and 2×4 at the UE, with 4 dBm transmit power at the gNB. Noise power spectral density of -174 dBm/Hz and noise figure of 5 dB are considered. Only downlink UDP (User Datagram Protocol) traffic is simulated, in which, one packet (with size of 100 Bytes) every 200 ms is sent over a period of 50 s. The Radio Link Control (RLC) is used in unacknowledged mode (UM). Two slots of PHY-MAC processing delay (i.e., 250 us) and 100 us of decoding latency are considered. We update the channel every 150 ms so that every packet encounters a different channel realization, thus getting statistical significance with respect to the fading.

For the performance metrics, the end-to-end delay of UDP packets ('delay' in ms), the packet loss at application layer ('APP loss' in %), and transmission data failures at PHY layer ('PHY loss' in %) are collected. Since higher packet losses are expected with increasing the gNB-UE distance, to alleviate the impact of the RLC UM timers on the end-to-end delay, the RLC UM is configured with a reordering window timer of 10

[1]NR allows rate matching to vary code block sizes slightly to assure code blocks align on OFDM symbol boundaries.